



Physicochemical properties of ceramic tape involving $\text{Ca}_{0.05}\text{Ba}_{0.95}\text{Ce}_{0.9}\text{Y}_{0.1}\text{O}_3$ as an electrolyte designed for electrolyte-supported solid oxide fuel cells (IT-SOFCs)

Bartłomiej Lis¹ · Magdalena Dudek¹ · Ryszard Kluczowski² · Mariusz Krauz² · Michał Kawalec² · Michał Mosiałek³ · Radosław Lach⁴

Received: 30 July 2017 / Accepted: 23 February 2018 / Published online: 3 March 2018
© Akadémiai Kiadó, Budapest, Hungary 2018

Abstract

A proton-conducting membrane involving modified barium cerate $\text{BaCe}_{0.9}\text{Y}_{0.1}\text{O}_3$ was obtained in the form of gas-tight ceramic tape. Monophase $\text{Ca}_{0.05}\text{Ba}_{0.95}\text{Ce}_{0.9}\text{Y}_{0.1}\text{O}_3$ (5CBCY) powder and an organic medium consisting of polyvinyl butyral used as a binder, a plasticiser based on carboxylic acid esters, and a mixture of ethanol and methyl ethyl ketone were used to prepare slurry for the tape-casting process. Gas-tight ceramic tapes involving 5CBCY and sintered samples were tested as electrolytes in hydrogen–oxygen button solid oxide fuel cells within the temperature range 500–750 °C. Variations in OCV and ohmic resistance (R_s) were determined within this range. A considerable decrease in R_s value was recorded for 5CBCY tape compared to 5CBCY sintered samples. A series of symmetrical cells with 5CBCY electrolytes was analysed. The lowest ASR values for the investigated cells were found for a newly elaborated LSCF–5CBCY cathode as well as for a Ni–5CBCY anode. These electrode materials appear to be suitable for 5CBCY-electrolyte-supported solid oxide fuel cells.

Keywords Solid oxide fuel cells · Ceramic tape · Ceramic proton conductor · $\text{BaCe}_{0.9}\text{Y}_{0.1}\text{O}_3$

✉ Magdalena Dudek
potoczek@agh.edu.pl

Bartłomiej Lis
blis@agh.edu.pl

Ryszard Kluczowski
kluczowski@cerel.pl

Michał Kawalec
kawalec@cerel.pl

Michał Mosiałek
nbmosial@agh.edu.pl

Radosław Lach
radek.lach@poczta.fm

¹ Faculty of Fuels and Energy, AGH-University of Science and Technology, Av. Mickiewicza 30, 30-059 Cracow, Poland

² Ceramic Department CEREL, Institute of Power Engineering, Techniczna 1 St, 36-040 Boguchwała, Poland

³ PAN Jerzy Haber Institute of Catalysis and Surface Chemistry, Polish Academy of Science, Niezapominajek 8, 30-239 Krakow, Poland

⁴ Faculty of Materials Science and Ceramics, AGH-University of Science and Technology, Av. Mickiewicza, 30-059 Cracow, Poland

Introduction

Since Iwahara's 1980 discovery of the high-temperature ceramic proton conductivity of BaCeO_3 -based materials, there has been growing interest in certain perovskite oxides, based on their potential application as proton-conducting ceramic membranes in electrochemical devices such as solid oxide fuel cells, solid oxide electrolyzers, reactors for the oxidative dehydrogenation of certain organic compounds, and gas sensors for monitoring hydrogen in gas atmospheres [1–4]. In general, the doped cerates $\text{MCE}_{1-x}\text{Y}_x\text{O}_{3-\delta}$, $\text{M} = \text{Ba}^{2+}$ or Sr^{2+} , exhibited higher electrical conductivity but limited chemical stability in CO_2 or H_2O gas atmospheres when compared, respectively, to the zirconates $\text{MZr}_{1-x}\text{Y}_x\text{O}_3$, Ba^{2+} and Sr^{2+} , where: $0 < x < 0.2$ [5–7]. Nowadays, research in the field of SOFCs is focused mainly on an intermediate temperature (IT) range of 500–750 °C. In SOFCs with oxide electrolytes, water is produced on the anode side, which dilutes the fuel. Ceramic proton conductors based on $\text{BaCe}_{1-x}\text{Y}_x\text{O}_3$, $0 < x < 0.3$, appear to be valuable

components for developing cost-effective SOFCs operating within an IT range of 500–700 °C. Protons are characterised by greater mobility than oxygen ions because of their much smaller size. The diffusion of protons is also much less temperature dependent than that of oxygen ions. Therefore, at lower temperatures, it is potentially easier to obtain greater conductivity for proton conductors than for oxygen ion conductors. This provides a strong incentive (as well as the potential) to lower electrical resistivity and to improve chemical stability in gas atmospheres involving CO₂ or H₂O [8, 9]. Previously, it had been found that the partial substitution of barium for calcium in (Ba_{1-x}Ca_x)(M_{0.9}Y_{0.1})O₃ solid solutions, where M = Ce, Zr and 0 < x < 0.1, led to an improvement in electrical conductivity compared to initial BaM_{0.9}Y_{0.1}O₃, M = Ce, Zr, samples [10].

Some potential strategic actions were elaborated to improve the physicochemical properties of BaCeO₃-based materials [11–13]. It was found that the introduction of strontium into Ba_{1-x}Sr_xCe_{0.9}Y_{0.1}O₃, where 0 < x < 0.2, led to a small decrease in ionic conductivity compared to the initial BaCe_{0.9}Y_{0.1}O₃ material, but improved chemical stability in gas atmospheres involving CO₂ or water [14, 15]. An elaborated method involving the fabrication of a thin layer of proton-conducting ceramic appears to be one possible way to lower electrical resistance. Tape casting is a low-cost process particularly well suited for the fabrication of thin (100–1000 μm) flat components for solid oxide fuel cells, enabling the production of a wide variety of controlled morphologies, from highly porous to fully dense microstructures such as electrodes and electrolytes [16–19]. It is widely known that a planar electrolyte-supported SOFC constitutes an attractive geometry for an SOFC stack configuration for which relatively large and flat cell components are required [20, 21].

Costa et al. [22] investigated the potential for forming BaCe_{0.9}Y_{0.1}O₃ ceramic tapes using aqueous or non-aqueous slurries. It was found that a water-based system was unsuitable for manufacturing ceramic tapes involving barium cerate due to a strong tendency towards rapid hydrolysis. On the other hand, the application of a tape-casting system involving an organic medium enabled the fabrication of a BaCe_{0.9}Y_{0.1}O₃ electrolyte as well as NiO–BaCe_{0.9}Y_{0.1}O₃ anode-based materials. The analysis of the results is limited to X-ray diffraction analysis and SEM observation of the obtained materials. The literature is lacking in data reflecting the analysis of physicochemical properties of BaCeO₃-based ceramic tape crucial for application as an electrolyte support in the construction of an intermediate temperature solid oxide fuel cell.

The aim of this study was to elaborate an organic tape-casting method for the fabrication of ceramic tape involving a Ba_{0.95}Ca_{0.05}Ce_{0.9}Y_{0.1}O₃ membrane as a

component of an electrolyte-supported SOFC. Special attention was paid to: (1) determining the physicochemical properties of BaCeO₃-based tape; (2) elaborating cathode and anode composite materials suitable for the construction of a Ba_{0.95}Ca_{0.05}Ce_{0.9}Y_{0.1}O₃-tape electrolyte-supported solid oxide fuel cell which could be operated in the temperature range 500–750 °C.

Experimental

Ba_{0.95}Ca_{0.05}Ce_{0.9}Y_{0.1}O₃ powder preparation

Ba_{0.95}Ca_{0.05}Ce_{0.9}Y_{0.1}O₃ (hereafter: 5CBCY) monophase powder was synthesised by means of a solid-state reaction. The starting reagents used to synthesise 5CBCY powder were barium carbonate and calcium carbonate (Avantor Performance Material Poland S.A, p.a.), yttrium(III) oxide (Sigma-Aldrich, 99.99%), and cerium oxide (Acros Organics, 99.9%). Stoichiometric amounts corresponding to the formula Ba_{0.95}Ca_{0.05}Ce_{0.9}Y_{0.1}O₃ were homogenised and milled in a planetary ball mill (Retsch PM 100). A small portion of mixed reagents corresponding to the formula Ba_{0.95}Ca_{0.05}Ce_{0.9}Y_{0.1}O₃ was calcined within a temperature range of 900–1150 °C for 2 h. Following calcination, analysis of phase composition was performed using X-ray diffraction analysis. The monophase of 5CBCY was found at a temperature of 1150 °C. It was decided to synthesise a 200-g portion of powder at 1200 °C for 2 h. The 5CBCY powder was ground in dry ethanol with zirconia grinding media.

Preparation of slurry and 5CBCY ceramic tapes

The organic medium used for tape casting included polyvinyl butyral (Kuraray Europe GmbH) used as a binder, a plasticiser based on carboxylic acid esters (Zschimmer & Schwarz), and a mixture of ethanol (Avantor Performance Material Poland S.A, p.a.) and methyl ethyl ketone (Chempur, Poland) used as a solvent. The 5CBCY powder was mixed in a polythene container with an organic medium at a mass ratio of 54:46, attaining the form of slurry, which was then mixed and ground by means of ball milling to ensure homogenisation and destruction of agglomerates. The grinding process proceeded for 24 h, using high-speed rollers. The resulting slurry underwent deaeration for 24 h at a reduced rotation speed and subsequently for 2 min in low-pressure conditions. Then the slurry was transferred to a tape-casting device. The gap between the ‘doctor blade’ (cast squeegee) and tape-casting table surface amounted to 0.8 mm. Green tape was cast at the rate of 2 cm s⁻¹ on a PTFE surface covered with anti-adhesive coating. Subsequently, the tape was dried in an air-conditioned room for

24 h. After the drying process, the thickness of the tape was 0.28 mm. At this stage, 28-mm disc-shaped samples were laser-cut from the tape. The 5CBCY samples were sintered within a temperature range of 1450–1600 °C. The 5CBCY ceramic tapes characterised by the highest relative density were selected for further investigations.

Electrochemical investigations of 5CBCY ceramic electrolytes in symmetrical solid oxide cells and in hydrogen–oxygen solid oxide fuel cells

The following single-button solid oxide cells were investigated:

1. H_2 , Pt|5CBCY|Pt, O_2
2. O_2 , LSCF|5CBCY|LSCF, O_2
3. O_2 , LSCF–GDC|5CBCY|LSCF–GDC, O_2
4. O_2 , LSCF–5CBCY|5CBCY|LSCF–5CBCY, O_2
5. H_2 , Ni–5CBCY|5CBCY|Ni–5CBCY, H_2

In the case of cell (1), the 5CBCY electrolyte was manufactured in the shape of discs (diameter ~ 20 mm), but differences in thickness were applied in this study: 5CBCY ceramic tape with a thickness of 0.14 mm (hereafter: 5CBCY-T), and disc-shaped sintered samples with a thickness of 1.4 mm (hereafter: 5CBCY-S). Porous platinum electrodes (the active surface of each electrode equalled about 1.3 cm^2) were applied in the initial electrochemical tests described in this paper. The electrodes were screen-printed from commercial Pt paste. Electrolytes with Pt electrodes were heated at 1000 °C for 1 h to obtain porous forms for both electrodes.

$(\text{La}_{0.60}\text{Sr}_{0.40})_{0.95}\text{Co}_{0.20}\text{Fe}_{0.80}\text{O}_{3-\delta}$ (LSCF) was chosen from the group of oxide cathode materials for this investigation of the potential of prepared optimised cathode materials for an electrolyte-supported IT-SOFC with a 5CBCY electrolyte. Although LSCF is known to be a good cathode material for an IT-SOFC with a ceramic oxide electrolyte, some authors have reported that it also seems to be a promising cathode for SOFCs with a ceramic proton-conducting membrane [23, 24]. The electrochemical behaviour of an LSCF|5CBCY interface under prolonged cathodic polarisation was investigated. Two kinds of LSCF electrode were applied in this study. In the first case, a quasi-point electrode was made from dense sintered LSCF. The LSCF samples were prepared from commercial powders supplied by Fuel Cell Materials, USA. The pellets were isostatically pressed under 250 MPa and sintered at a temperature of 1200 °C for 24 h. LSCF cathodes were formed from previously sintered samples in the shape of pyramids by means of a circular saw and diamond files. LSCF quasi-point electrodes were placed along with a 5CBCY ceramic electrolyte in a custom-designed, hand-made electrochemical setup [25, 26]. Only the end of the

pyramid pointed at the cathode was placed in contact with the electrolyte. Electrochemical measurements of an LSCF|5CBCY system under prolonged polarisation, under negative potential from -0.05 to -0.7 V, were performed in air at 700 °C for 100 h. A porous monophase LSCF cathode and an LSCF–GDC cathode (thickness $\sim 35\ \mu\text{m}$) were manufactured using the screen printing method. Commercial LSCF or LSCF–GDC paste was screen-printed on both sides of the electrolyte sample and then sintered at 1200 °C for 2 h with a heating and cooling rate of $1\ \text{°C min}^{-1}$. A new composite LSCF–5CBCY cathode was also elaborated and investigated in this study. LSCF–5CBCY cathode composite paste was obtained by mixing equal equilibrium amounts of LSCF and 5CBCY powders in an agate mortar and then adding the organic carrier. The prepared paste was applied via screen printing to the 5CBCY electrolyte surface. An attempt to elaborate new Ni–5CBCY anode material for a 5CBCY electrolyte-supported IT-SOFC was also undertaken. Ni–5CBCY anode composite paste was prepared by mixing 5CBCY electrolyte powder with nickel oxide powder (Acros Organics) in an agate mortar. Subsequently, an organic carrier was added and ground to a homogeneous consistency. The prepared paste was applied by screen printing to the 5CBCY electrolyte surface. The anode was heated at 1400 °C for 4 h in air. In this way, a series of symmetrical solid oxide fuel cells (2)–(5) with 5CBCY tape were obtained.

Symmetrical button solid oxide fuel cells (2)–(5) with porous LSCF, LSCF–GDC, and LSCF–5CBCY cathodes were used to determine polarisation resistance R_p and area specific resistance ASR within the temperature range 550–700 °C.

Electrochemical measurements were performed using a Solartron SI 1287 Electrochemical Interface with a 1255B Frequency Response Analyzer. Measurements were performed in dry and wet air for cell (2) with LSCF electrodes. The amplitude of the sinusoidal voltage signal was 10 mV. The Minuit [27, 28] program was used to fit the parameters of the equation describing the assumed equivalent electrical circuit (EEC).

Analytical methods of evaluation of the physicochemical properties of a 5CBCY electrolyte prepared in the form of powder and as a ceramic tape

XRD measurements with a PANalytical Empyrean system employing monochromatic $\text{CuK}\alpha$ radiation was used to determine the phase composition to determine the phase composition of 5CBCY applied powder, sintered ceramic tape, an LSCF–5CBCY composite cathode, and Ni–5CBCY anode material. The lattice parameters of all

investigated materials were determined using the Rietveld method. The morphology of 5CBCY particles was then observed using scanning electron microscopy (SEM). Ultra-high-resolution scanning electron microscopy with a Nova NanoSEM 200 (FEI Europe) was used for all SEM observations.

The particle size distribution of ground 5CBCY powder was determined in an ethanol suspension with a Mastersizer 2000 (Malvern Instruments) laser particle size analyser. The surface area of the powder was determined using the isotherm BET method (Nova 1200e, Quantachrome Instruments). The powder was subsequently applied to the preparation of slurry for the tape-casting process.

Thermal analysis (TGA-DTA, STA 449 F3 Jupiter thermal analyser, NETZSCH, USA) was used to determine the thermal effect occurring during the heating of green tape prepared from 5CBCY within a temperature range of 20–1000 °C. The measurements were performed in air; a ramp of 10 °C min⁻¹ was applied. Confocal microscopy (Olympus LEXT OLS4000) was used to observe the surface of the 5CBCY tape before sintering. Dilatometry was used to determine the variations in the dimensions of samples heated within a temperature range of 25–1600 °C. The samples were measured using a NETZSCH model DIL 402. The density of 5CBCY samples was determined using the Archimedes' method. Scanning electron microscopy was used to observe the microstructure of 5CBCY tape sintered in air in a temperature range of 1450–1600 °C for 2 h. SEM observation was also carried out for the microstructure of the obtained LSCF, LSCF–5CBCY, and Ni–5CBCY electrodes as well as for a cross section of the 5CBCY sintered ceramic tape and cross sections of all investigated SOFC cells.

Results

Figure 1a presents the XRD patterns recorded for 5CBCY powder following calcination at 1200 °C for 2 h and for samples formed from this powder sintered at 1500 °C for 2 h. The increase in heating temperature to 1500 °C caused the characteristic reflections of BaCeO₃ to become stronger in terms of intensity compared to those calcined at 1200 °C. In a comparative analysis of the XRD diffraction patterns of 5CBCY recorded both for powder (A) and for sintered and isostatically pressed samples of 5CBCY powders (B), no considerable differences were observed. On the basis of X-ray investigations and Rietveld analysis, it was found that the obtained solid solutions of Ba_{0.95}Ca_{0.05}Ce_{0.9}Y_{0.1}O₃ crystallise in rhombohedral structure in the space group *R3c*; however, the presence of a trace amount of BaCe_{0.9}Y_{0.1}O₃ orthorhombic phase cannot be excluded. Figure 1b shows the X-ray diffraction patterns

recorded for an LSCF cathode (C), 5CBCY tape sintered at 1600 °C (D), and LSCF–5CBCY composite cathodes (E). The recorded XRD pattern for (C) reflects monophase LSCF cathode material [29, 30]. In Fig. 1b, an XRD pattern was also recorded for an LSCF–5CBCY composite cathode. The introduction to LSCF of 5CBCY as a second phase, aimed at the preparation of a composite cathode and its thermal treatment at 1200 °C for 2 h caused an increase in the lattice parameters of LSCF material compared to the monophase cathode previously shown in XRD pattern (C). The analysis of XRD patterns (C) and (D) showed LSCF as possessing hexagonal symmetry. Based on the XRD pattern recorded for the LSCF sample (C) only, the calculated lattice parameters were $a = b = 5.494$ Å, and $c = 13.411$ Å. In the case of the LSCF–5CBCY composite cathode, an increase in lattice parameters to $a = b = 5.5076$ Å was recorded. Lattice parameter c also increased, to 13.4128 Å. The observed phenomena indicated the mutual reactivity between the LSCF and 5CBCY components of composite cathodes. There is no data existing in the literature explaining the possible mechanism of chemical reactivity between LSCF and 5CBCY components. The increase in the a and b lattice parameters can be directly attributed to the diffusion of (barium or calcium) cations from Ba_{0.95}Ca_{0.05}Ce_{0.9}Y_{0.1}O₃ into LSCF perovskite during high-temperature treatment. These facts caused the enrichment of the LSCF cathode with calcium or barium and a consequent reduction in the concentration of these elements in the Ba_{0.95}Ca_{0.05}Ce_{0.9}Y_{0.1}O₃ electrolyte. It was previously found that increase of deficiency in Ba_{1-x}Ce_{0.9}Y_{0.1}O₃ can lead to variation in the symmetry of the crystal structure of BCY [14, 31, 32]. These statements are in close agreement with the observed regular symmetry of Ba_{0.95}Ca_{0.05}Ce_{0.9}Y_{0.1}O₃ in the XRD pattern.

The physicochemical properties of ceramic powder used to prepare slurry for tape casting are crucial for obtaining high-quality green tape (i.e. smooth, no cracks, no disparities in thickness). The ceramic powder must be homogeneously dispersed in the slurry. Important factors include particle sizes and surface area. A narrow particle size distribution is crucial for ceramic tape casting, as it prevents grain segregation while the green tape is drying. Uneven grain distribution in green tape leads to the formation of defects at the sintering stage. The particle size distribution of the 5CBCY powder used is presented, along with its morphology, in Fig. 2a, b.

The dependence of particle sizes (Fig. 2a) on volume indicated that this distribution is rather narrow: 80 vol% of all 5CBCY particles range in size from 2.42 to 20.99 μm. The parameters D₁₀ (2.42 μm), D₅₀ (5.64 μm), and D₉₀ (20.92 μm), determined by means of particle size analysis, were also calculated. Analysis of SEM images (Fig. 2b)

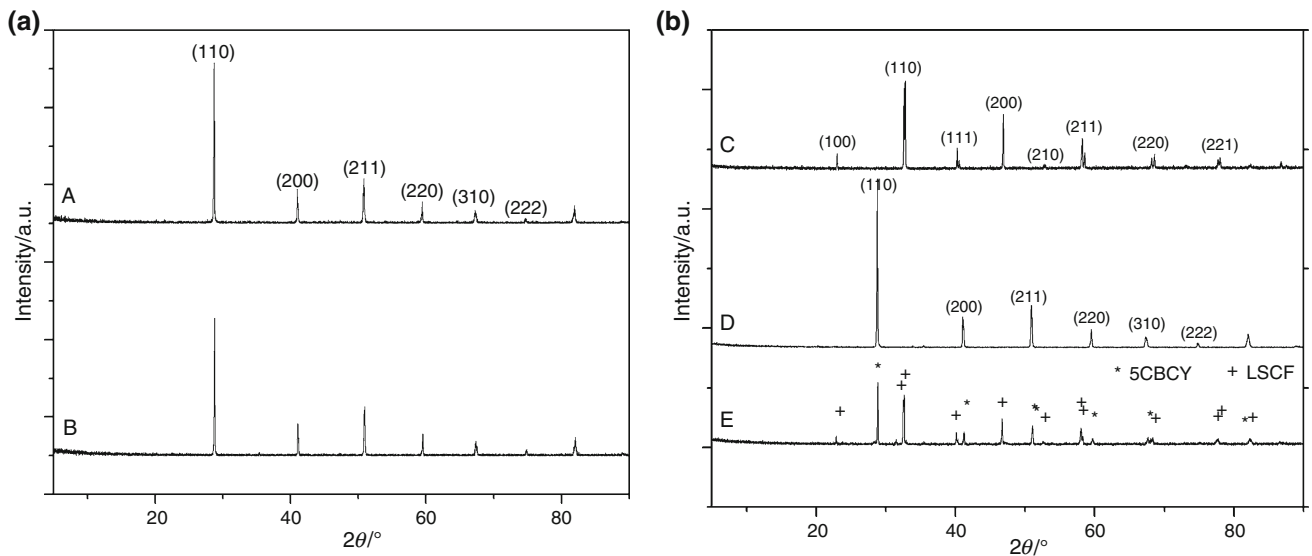


Fig. 1 a X-ray diffraction pattern recorded for 5CBCY powder (A) and ceramic tape (B), b X-ray diffraction pattern recorded for LSCF (C), 5CBCY (sintered sample–D) and LSCF–5CBCY commonly heated samples at 1200 °C for 2 h (E)

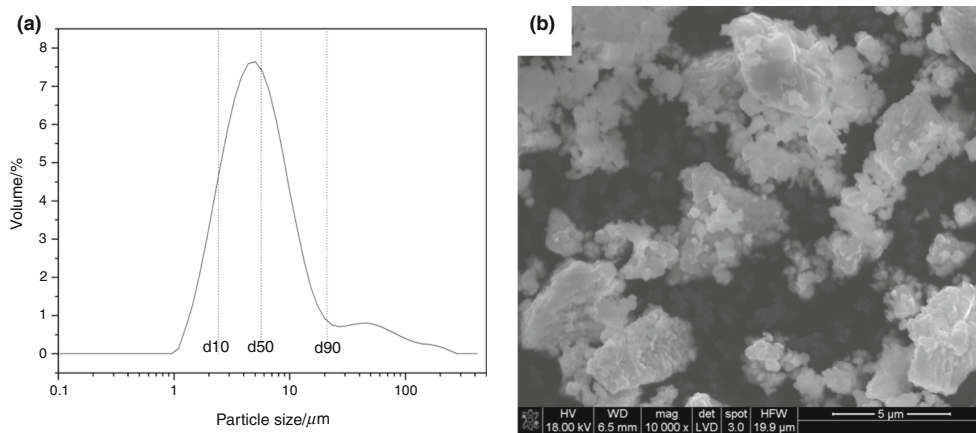


Fig. 2 Distribution of particle sizes for 5CBCY powder used in the tape-casting process (a) and The SEM image of 5CBCY powder (b)

shows that 5CBCY powders are characterised by isometric particle sizes ranging from 0.5 to 20 μm .

The same form of agglomerates was observed using SEM. The data obtained from laser measurements are in close agreement with the SEM analysis. The isometric shape of 5CBCY particles and their narrow size distribution are favourable for the preparation of slurry for casting.

The obtained green tape was flat and flexible. Confocal microscopy (Fig. 3) was used to inspect the surface of the tape. As can be seen, this observation confirmed that the surface was flat and that no defects were to be found. No differences in thickness or roughness were noted during

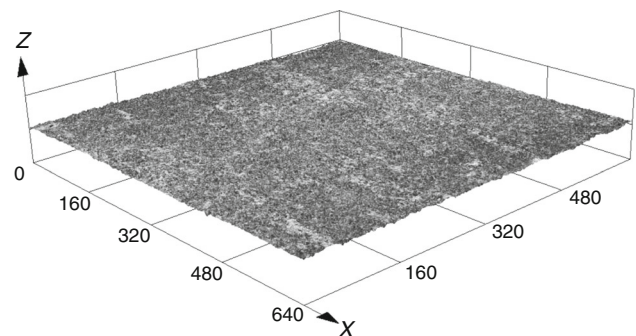


Fig. 3 Confocal image for the surface of 5CBCY green tape

inspection of the fabricated tape. The presented results confirmed that the applied synthesis and grinding conditions for preparing the 5CBCY powder and selected organic binder enabled the acquisition of defect-free 5CBCY ceramic tape.

During the sintering process, 5CBCY green tape was subjected to the irreversible variation that occurs with an increase from room temperature to the final heating temperature. Knowledge of the thermal effects which occur during temperature increases is necessary for the elaboration of suitable sintering conditions in order to release the organic medium from the ceramic part, to reduce porosity, and to obtain gas-tight samples without cracks or certain defects.

The DTA and TG curves recorded for 5CBCY green tape in air within the temperature range 25–1000 °C are presented in Fig. 4. Analysis of DTA and TG curves indicated small mass losses on the latter within the temperature range 25–250 °C. These may be directly related to solvent evaporation. The first recorded thermal effect on the DTA curve is narrow, with one high-intensity exothermic peak at 346 °C and another small exothermic peak at 463 °C. These peaks may be directly connected with the thermal decomposition of organic binders. Above 470 °C up to 1000 °C, there was a constant mass loss recorded by TG (~ 5%).

Figure 5 shows the densification behaviour of 5CBCY ceramic tape heated at a constant rate of 5 °C min⁻¹ within a temperature range of 25–1550 °C. Sintering of ceramic tapes started at a temperature of about 1308 °C. Up to 1550 °C shrinkage of 17.4% was measured for 5CBCY tape. The recorded data from dilatometry measurements agree closely with the results obtained from density measurements. The relative density of 5CBCY ceramic tape at a temperature of 1550 °C reached 95% of theoretical

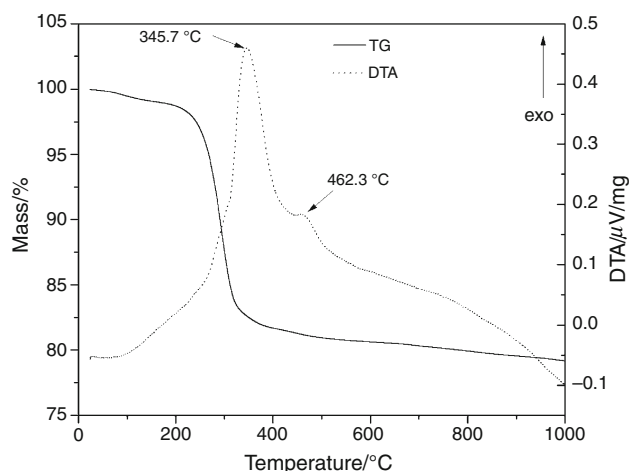


Fig. 4 DTA and TG curves recorded for a 5CBCY ceramic tape

density. An increase in relative density up to 98% was found for a 5CBCY sample sintered at 1600 °C.

A ceramic electrolyte designed for planar SOFC application should be contained in flat and dense tape with a homogenous microstructure. Electrolytes for SOFC application require a relative density above 95 wt%. The presence of porosity leads to a decrease in ionic conductivity and the mechanical properties of ceramic shapes.

SEM observation of a sintered 5CBCY sample at 1600 °C for 2 h and of a cross section of the symmetrical cell LSCF|5CBCY|LSCF (Fig. 6a, b) was also conducted. The sintered 5CBCY tape was characterised by a uniform microstructure with rather isometric grains, 5–10 μm. Figure 6b reflects a dense electrolyte layer with a thickness of approximately 170–200 μm. Negligible porosity was noted in the observed cross section of the 5CBCY electrolyte. Strong adhesion of LSCF layers (~ 35 μm) was observed on both sides of the 5CBCY tapes. Figure 6c shows images of newly prepared NiO-5CBY|5CBCY|NiO-5CBY anode materials. Porous anode layers without delamination were obtained on both sides of the dense 5CBCY electrolyte.

Elaborated gas-tight Ba_{0.95}Ca_{0.05}Ce_{0.9}Y_{0.1}O₃ (5CBCY) ceramic tape was first tested as an electrolyte in a hydrogen–oxygen solid oxide fuel cell (cell 1) operating within the temperature range 400–800 °C. Figure 7 presents the dependence on temperature of the open-circuit voltage (OCV) recorded for an SOFC with a 5CBCY electrolyte. In this graph, two different measurement series of the OCVs obtained for an SOFC with a 5CBCY electrolyte were analysed: involving, first, 5CBCY ceramic tape (~ 0.16 mm) within the temperature range 500–750 °C, and second, a 5CBCY sintered sample as an electrolyte (thickness: 1.4 mm).

All measurements were performed in analogous conditions. OCV values calculated using the Nernst equation were also included in the graph. Analysis of these values within the temperature range 450–750 °C indicated a correlation between a slight decrease in OCV values and increasing temperatures. Within a temperature range of 500–600 °C, the OCV of cell (1) reached values slightly higher than 1 V. The measured values of OCV from the Pt|5CBCY|Pt cell within the temperature range 500–600 °C in series (1) and (2) were very close to 1 V. A decrease in OCV values was observed within a higher temperature range, i.e. 650–750 °C. In other research, Z. Sun et al. also recorded a decrease of OCV values for a hydrogen–oxygen SOFC with BaZr_{0.9}Y_{0.1}O₃ or BaZr_{0.9}Y_{0.1}O₃ with a calcia addition in the temperature range 500–700 °C. In the case of Pt|BaZr_{0.9}Y_{0.1}O₃|Pt or Pt|BaZr_{0.9}Y_{0.1}O₃ + 4% mol CaO|Pt SOFC cells, a marked tendency towards a decrease in OCV values was also observed at temperatures higher than 600 °C. An increase in electron–hole conduction in

Fig. 5 Thermal expansion and rate of expansion of 5CBCY green tape

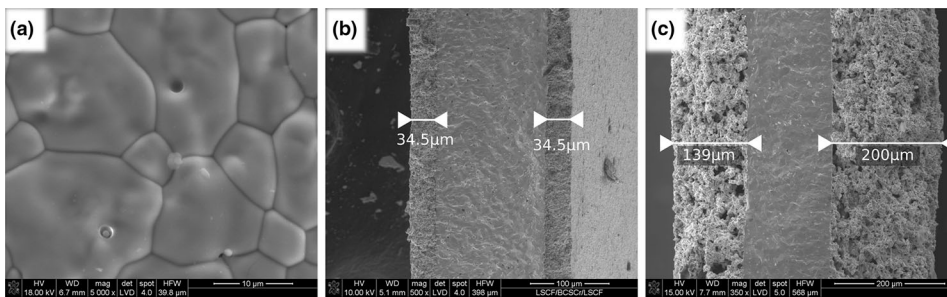
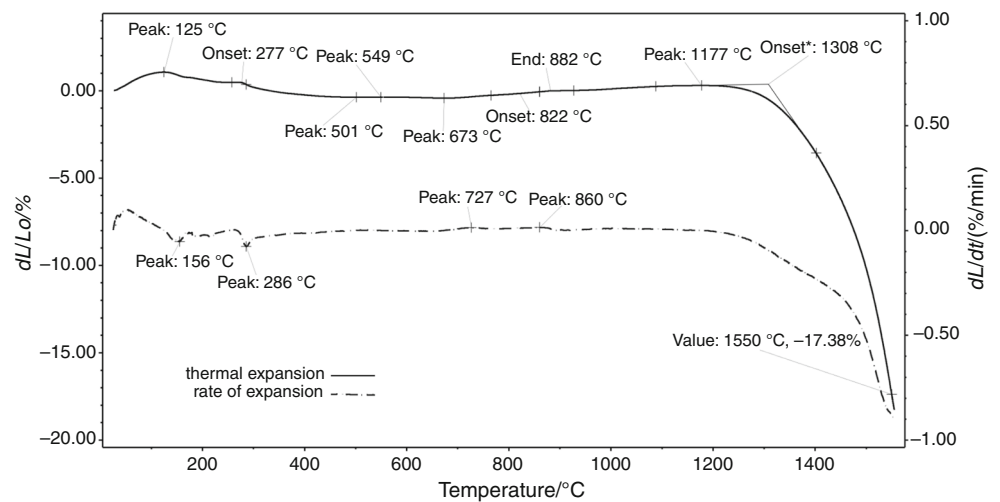


Fig. 6 a–c SEM image of microstructure of a 5CBCY tape sintered at 1600 °C for 2 h (a) and cross section: LSCF|5CBCY|LSCF (b) and Ni-5CBCY|5CBCY|Ni-5CBCY (c) solid oxide cells

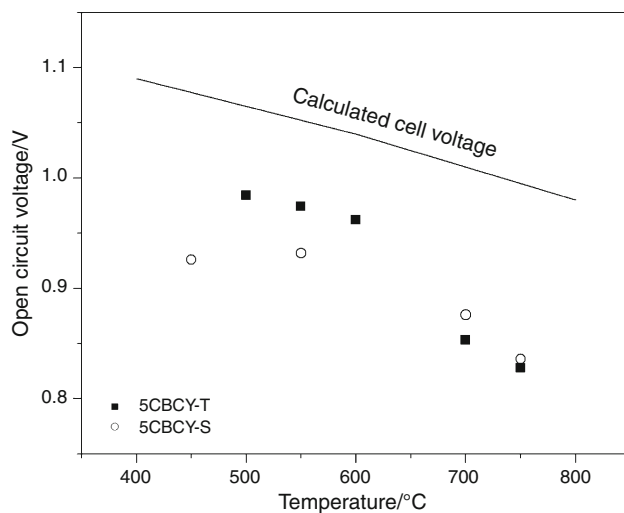


Fig. 7 Dependence of the open circuit voltage (OCV) of cell (1) versus temperature, recorded within temperature range of 500–750 °C

BaZrO_3 -based electrolytes in an air atmosphere at higher temperatures was pointed out as the main reason for the

reduced OCVs in the investigated cells. In the case of the $\text{Pt|BaZr}_{0.9}\text{Y}_{0.1}\text{O}_3 + 4\% \text{mol CaO|Pt}$ cell, an OCV value of about 0.93 V was recorded at 700 °C, compared to 0.99 V at 500 °C [33, 34]. Very similar values of OCV were reached for a Pt|5CBCY|Pt cell at the above-mentioned temperatures. In the case of BaCeO_3 -based materials, the OCV drop may result as well from a decrease in the ionic transport number at higher conductivity due to a possible increase in partial electronic conductivity.

Based on the initial electrochemical investigations of an IT-SOFC involving a 5CBCY electrolyte, the high values of OCV obtained for cell (1) also confirmed the gas-tightness of the electrolyte manufactured in the form of ceramic tape as well as in that of a pressed and sintered sample.

Electrochemical impedance spectroscopy (EIS) enabled determination of the comparative ohmic resistance R_s of a hydrogen–oxygen SOFC involving 5CBCY sintered ceramic tape and a 5CBCY sintered disc sample as electrolytes. Based on the analysis of data obtained via EIS measurement (Fig. 8), it was found that the R_s in SOFC (1),

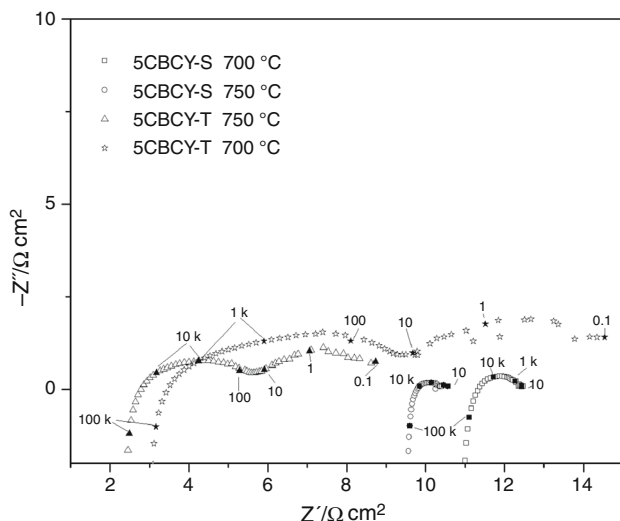


Fig. 8 EIS spectra recorded for cell (1) involving an 5CBCY-T or 5CBCY-S at 700 °C in dry air

involving a ceramic electrolyte with 5CBCY ceramic tape at 700 °C, was significantly lower than in an SOFC with the same electrolyte in the form of shaped discs. The obtained EIS spectra presented in Fig. 8 consist of a high-frequency (HF) inductive part and one or more depressed semicircles. The HF real-axis intercept of the spectra was assumed as the value of R_s .

An increase in temperature also reduced the ohmic resistance R_s of a single SOFC cell (1). Figure 9 presents the relationship between ohmic resistance R_s and temperature for cell (1) involving 5CBCY ceramic tape or a 5CBCY sintered sample. A reduction in the thickness of the 5CBCY electrolyte considerably reduced the ohmic resistance of cell (1) in the investigated temperature range of 400–750 °C.

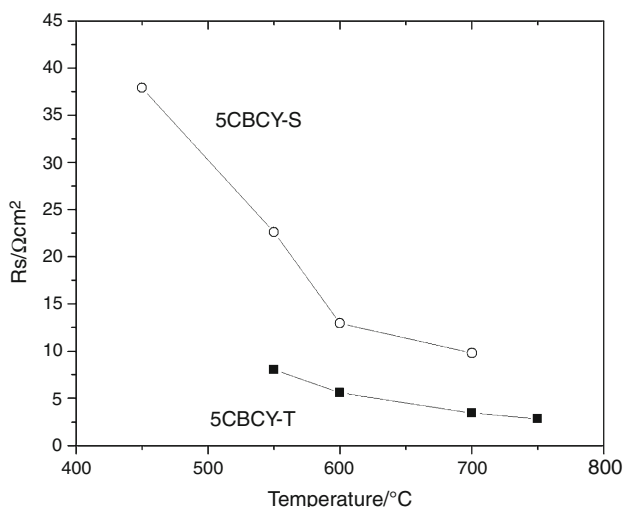


Fig. 9 Variation of ohmic resistance R_s determined using EIS method for cell (1) within in temperature range of 500–750 °C

One of the strategic goals leading to the improved performance of a SOFC with a 5CBCY electrolyte should be the identification of a suitable cathode material. The oxygen reduction reaction (ORR) occurring at the cathode of a SOFC causes most of the energy losses, leading in turn to a reduction in the cell’s energy efficiency. In the case of a ceramic fuel cell with a proton ceramic membrane, water is formed on the cathode side, complicating the cathode reaction mechanism and resulting in a higher level of polarisation resistance in the cathode. Although significant efforts have been exerted towards developing suitable cathodes for ceramic fuel cells with proton-conducting membranes (PCFCs), the problem of selecting an optimum cathode material has not yet been solved. Information describing the electrochemical behaviour of an LSCF cathode under long-term cathodic polarisation is lacking. In this study, quasi-point electrodes as well as classical porous LSCF electrodes were applied.

In this study, the impact of the electrochemical behaviours of a quasi-point LSCF and a porous cathode on polarisation over a range from -0.05 to -0.7 V at 700 °C was studied using the chronoamperometric method (CA). The typical dependencies of the currents flowing through the LSCF electrode at negative step polarisation $E = -0.05$ to -0.60 V recorded for a 5CBCY sample at 700 °C in dry air are depicted in Fig. 10. Generally, within the applied potential range (from -0.05 to -0.5 V), the current reached a fairly stable value over time for both types of applied electrodes. The impedance spectra (Fig. 11) before and after polarisation are almost identical, showing that polarisation did not affect the electrode’s properties.

The impedance spectra obtained for symmetrical cells (2) can be divided into up to four partially overlapping capacitive semicircles. Low- and medium-frequency semicircles usually depend on oxygen partial pressure, which can be ascribed to processes connected to the ORR, whereas high-frequency semicircles are associated with electrolyte conductivity. Capacitive arcs are represented in an EEC by a capacitor and resistor connected in parallel (R, C). Capacitors are replaced by constant phase elements (CPEs) whose impedance can be expressed by the following formula [28]:

$$Z_{CPE_i} = \frac{1}{2\pi f_0 C_i} \left(\frac{f_0}{jf} \right)^\alpha, \tag{1}$$

where i is the index denoting the various elements in the EEC in question; j is an imaginary unit; f is the frequency; f_0 is the frequency of reference, assumed to be 1 kHz; C_i is the capacitance at the frequency of reference; and α is a coefficient close to 1 for an ideal capacitor, usually assuming a value in the range 0.5–1.0. The impedance of an electrolyte is represented by the resistor R_0 . The applied

Fig. 10 Dependencies of the currents flowing through the LSCF quasi-point electrode (a) or porous electrode (b) at negative step polarisation $E = -0.05$ to -0.8 V recorded for a 5CBCY sample in dry air

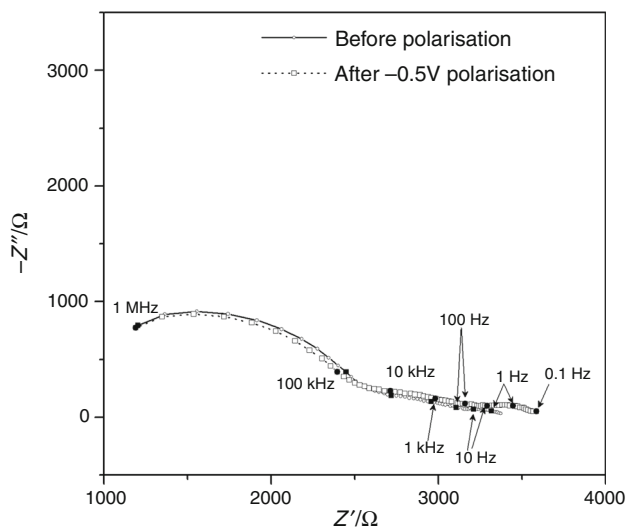
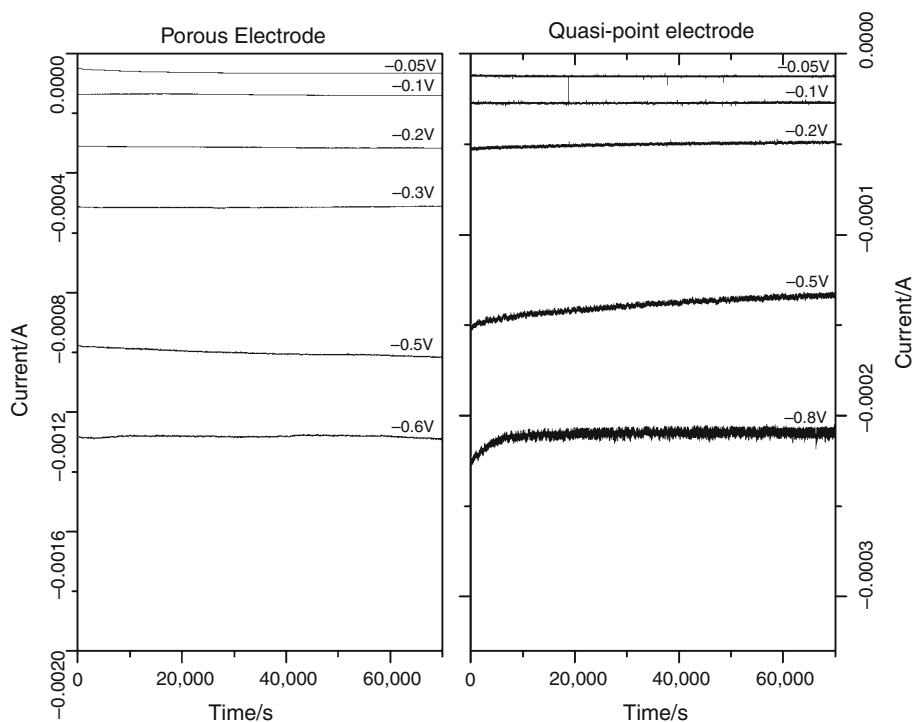


Fig. 11 Nyquist plots recorded for an LSCF/5CBCY system before and after applied polarisation at -0.5 V at 700 °C

EECs and a sample of recorded spectra are presented in Fig. 12.

The values of R_p for a BCY electrolyte are slightly higher than those reported in the paper [23]. This is, for the most part, directly connected with the electrolyte's greater thickness ($30\text{--}35$ μm), as well as with the architecture of the LSCF electrodes obtained in our studies, compared to the thickness ($4\text{--}5$ μm) of LSCF cathodes applied in the electrochemical studies described in the cited paper [23, 24]. The calculated ASR values vs temperature for

cells (2) and (3) are presented in Fig. 13. ASR resistance decreased with temperature in these cells. There was no observed difference in ASR values recorded between cells in dry and in wet air.

The electrochemical performance of the cathode follows the order $\text{LSCF-5CBCY} > \text{LSCF} > \text{LSCF-GDC}$. The enhanced performance of the LSCF-5CBCY composite cathode compared to the LSCF cathode can be ascribed mainly to the introduction of proton-/oxide-ion-conducting pathways. In the case of 5CBCY in dry air, oxide ion conductivity/electronic conductivity was observed. Composite cathodes involving MIECs, electrocatalysts, and oxygen ion conductors (O-composite cathodes) were also investigated for solid oxide fuel cells with proton-conducting membranes. He [35] found that the enhancement of electrochemical activity is the effect of addition of oxygen-ion conductor and could be attributed to the improvement on the surface exchange dynamics or providing the alternative oxygen diffusion path.

Some authors have reported that the electrochemical behaviour of LSCF- or SSC-infiltrated GDC O-composite electrodes in symmetrical cells exhibits lower polarisation resistance [36]. In this study, the introduction of the oxide-ion conductor GDC to the LSCF electrode did not lead to an improvement in performance compared to a monophasic LSCF electrode. The lowest ASR value in the investigated temperature range was observed at $550\text{--}700$ °C for the LSCF-5CBCY electrode. A decrease in cathode polarisation resistance was observed due to an increase in ionic

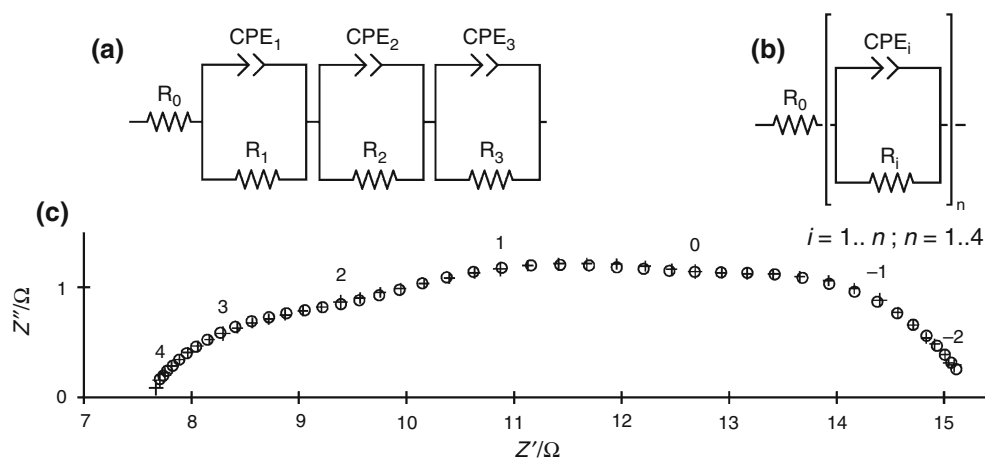


Fig. 12 Example of results of fitting applied EECs for 5CBCY ceramic tape of recorded spectra at 700 °C

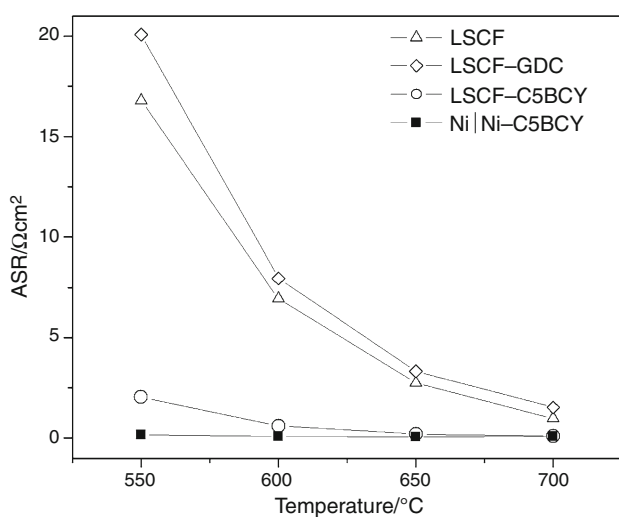


Fig. 13 Calculated ASR values versus temperature for cells (3–5) with 5CBCY-T

(oxide/proton) conductivity within a temperature range of 500–600 °C.

Figure 13 presents the ASR values determined for $H_2/Ni-5CBCY/5CBCY/Ni-5CBCY/H_2$ in the same temperature range. As can be seen, the elaborated Ni-5CBCY appears to be a suitable anode for an E-SOFC operating with a 5CBCY electrolyte. These results confirmed the actual potential for constructing a 5CBCY-electrolyte-supported SOFC with a LSCF-5CBCY cathode and a Ni-5CBCY anode.

Conclusions

Slurry for preparing a $Ba_{0.95}Ca_{0.05}Ce_{0.9}Y_{0.1}O_3$ ceramic tape was successfully obtained from monophasic ground 5CBCY powder originating from a solid-state reaction, in

combination with organic binders. Flat gas-tight 5CBCY ceramic tape was obtained after sintering at 1600 °C for 2 h in air. The uniform microstructure of the tape, with grains 1–10 μm, was observed with the use of SEM. The initial electrochemical tests performed on solid button oxide fuel cells confirmed the high quality of the prepared ceramic tape from the 5CBCY electrolytic material. The superiority of an IT-SOFC with 5CBCY ceramic tape, as opposed to 5CBCY disc samples, was proven. The ASR values obtained for a newly elaborated LSCF-5CBCY composite cathode are compatible with its application as a component of a 5CBCY electrolyte-supported solid oxide fuel cell. A Ni-5CBCY composite anode with lower ASR resistance was also elaborated.

Acknowledgements The paper was completed under a contract with the AGH University of Science and Technology, Cracow, Poland (No. 15.11.210.345). Some measurements were performed using scientific equipment belonging to the laboratories of the AGH-UST Energy Centre, Cracow, Poland.

References

- Iwahra H, Asakura Y, Katahira K, Tanaka M. Prospects of hydrogen technology using proton-conducting ceramics. *Solid State Ionics*. 2004;168:299–310.
- Tao Z, Zhu Z, Wang H, Liu W. A stable $BaCeO_3$ -based proton conductor for intermediate-temperature solid oxide fuel cells. *J Power Sources*. 2010;195:3481–4.
- Sawant P, Warma S, Wani BN, Bharadwaj SR. Influence of synthesis route on morphology and conduction behavior of $BaCe_{0.8}Y_{0.2}O_{3-\delta}$. *J Therm Anal Calorim*. 2012;107:189–95.
- Gaweł R, Przybylski K, Vivami M. Resistance of composite materials based on $BaCeO_3$ against the corrosive effect of carbon dioxide and water vapour at intermediate fuel cell. *J Therm Anal Calorim*. 2014;116:895–903.
- Bučko MM, Dudek M. Structural and electrical properties of $(Ba_{1-x}Sr_x)(Zr_{0.9}M_{0.1})O_3$, $M = Y, La$ solid solution. *J Power Sources*. 2009;194:25–30.

6. Kochetova N, Animitsa A, Medvedev M, Demin A, Tsiakars P. Recent activity in the development of proton-conducting oxides for high temperature applications. *RSC Adv.* 2016;6:73222–68.
7. Amsif M, Marrero-López D, Ruiz-Morales JC, Savvin SN, Núñez P. The effect of Zn addition on the structure and transport properties of $\text{BaCe}_{0.9-x}\text{Zr}_x\text{Y}_{0.1}\text{O}_{3-\delta}$. *J Eur Ceram Soc.* 2014;34:1553–62.
8. Pasierb P, Gajerski R, Osiadly M, Łącz A. Application of DTA-TG-MS for determination of chemical stability of $\text{BaCeO}_{3-\delta}$ —based protonic conductors. *J Therm Anal Calorim.* 2014;117:683–91.
9. Hossain S, Abdallan AM, Noorazeen S, Azad A. A review on proton conducting electrolytes for clean energy and intermediate temperature-solid oxide fuel cells. *Renew Sust Energ Rev.* 2017;79:750–64.
10. Dudek M, Lis B, Rapacz-Kmita A, Gajek M, Raźniak A. Some observation on the synthesis and electrolytic properties of $(\text{Ba}_{1-x}\text{Ca}_x)(\text{M}_{0.9}\text{Y}_{0.1})\text{O}_3$ $\text{M} = \text{Ce, Zr}$ based samples modified with calcium. *Mater Sci Poland.* 2016;34:101–14.
11. Okiba T, Fujishiro F, Hashimoto T. Evaluation of kinetic stability against CO_2 and conducting property of $\text{BaCe}_{0.9-x}\text{Zr}_x\text{Y}_{0.1}\text{O}_{3-\delta}$. *J Therm Anal Calorim.* 2013;113:1269–74.
12. Radojković A, Žunić M, Savić SM, Branković G, Branković Z. Chemical stability and electrical properties of Nb doped $\text{BaCe}_{0.9}\text{Y}_{0.1}\text{O}_{3-\delta}$ as a high temperature proton conducting electrolyte for IT-SOFC. *Ceram Int.* 2013;29:2631–7.
13. Łącz A, Pasierb P. Synthesis and properties of $\text{BaCe}_{1-x}\text{Y}_x\text{O}_{3-\delta}$ — BaWO_4 composite protonic conductors. *J Therm Anal Calorim.* 2013;113:405–12.
14. Hung IM, Peng HW, Zheng SL, Lin CP, Wu JS. Phase stability and conductivity of $\text{Ba}_{1-x}\text{Sr}_x\text{Ce}_{0.9}\text{Y}_{0.1}\text{O}_{3-\delta}$ solid oxide fuel cell electrolyte. *J Power Sources.* 2009;193:155–9.
15. Wang S, Zhao F, Zhang L, Brinkman K, Chen F. Stability and electrical property of $\text{Ba}_{1-x}\text{Sr}_x\text{Ce}_{0.8}\text{Y}_{0.2}\text{O}_{3-\delta}$ high temperature proton conductor. *J Alloys Compd.* 2010;506:263–7.
16. Timakul P, Jinawath S, Aungkavattana P. Fabrication of electrolyte materials for solid oxide fuel cells by tape-casting. *Ceram Int.* 2008;34:867–71.
17. Fernández-González R, Molina T, Savvin S, Moreno R, Makradi A, Núñez P. Fabrication and electrical characterization of several YSZ tapes for SOFC application. *Ceram Int.* 2014;40:4253–14259.
18. Fu Y, Liu Y, Hu S. Aqueous tape casting and crystallization behaviour of gadolinia-doped ceria. *Ceram Int.* 2009;35:3153–9.
19. Mahmud LS, Muchtar A, Somalu MR. Challenges in fabricating planar solid oxide fuel cells: a review. *Renew Sust Energ Rev.* 2017;72:105–16.
20. Savignat SB, Chiron M, Barthet C. Tape casting of new electrolyte and anode materials for SOFCs operated at intermediate temperature. *J Eur Ceram.* 2007;27:673–8.
21. Zhou J, Liu Q, Zhang L, Chan SH. A study of short stack with large area solid oxide fuel cells by aqueous tape casting. *Int J Hydrog. Energy.* 2016;41:18203–6.
22. Costa R, Hafsaoui J, Oliviera A, Grosjean A, Caruel M, Chesnaud A, Thorel A. Tape casting of proton conducting material. *J Appl Electrochem.* 2009;36:485–95.
23. Yoo CY, Yun DS, Park SY, Park JH, Kwak M. Investigations of electrochemical properties of model lanthanum cobalt ferrite—based cathodes for proton ceramic fuel cells. *Electrocatalysis.* 2016;7:280–6.
24. Ii H, Choi S, Yoon KC, Son H, Kim BK, Lee H, Lee J. Influence of wet atmosphere on electrical and transport properties of lanthanum strontium cobalt ferrite cathode materials for protonic ceramic fuel cells. *Solid State Ionics.* 2013;249:249–50.
25. Raźniak A, Tomczyk P. Application of microelectrodes for investigation of the oxygen electrode reaction in selected electrolytes. *Mater Sci Poland.* 2008;26:195–206.
26. Tomczyk P, Żurek S, Mosialek M. Effect of time and polarization on kinetics of the oxygen electrode reaction at an Au/YSZ interface. *J Electroceram.* 2009;23:25–36.
27. James F, Roos M. Minuit—a system for function minimization and analysis of the parameter errors and correlations. *Comput Phys Commun.* 1975;10:343–67.
28. Mosialek M, Nowak P, Dudek M, Mordarski G. Oxygen reduction at the $\text{Ag/Gd}_{0.2}\text{Ce}_{0.8}\text{O}_{1.9}$ interface studied by electrochemical impedance spectroscopy and cyclic voltammetry at the silver point electrode. *Electrochim Acta.* 2014;120:248–53.
29. Chanquia CM, Mogni L, Troiani HE, Caneiro A. Highly active $\text{La}_{0.4}\text{Sr}_{0.6}\text{Co}_{0.8}\text{Fe}_{0.2}\text{O}_{3-\delta}$ nanocatalyst for oxygen reduction in intermediate temperature solid oxide fuel cells. *J Power Sources.* 2014;270:457–67.
30. Asadi AA, Behrouzifar A, Iravaninia M, Mohammedi T, Pak A. Preparation and oxygen permeation of $\text{La}_{0.6}\text{Sr}_{0.4}\text{Co}_{0.2}\text{Fe}_{0.8}\text{O}_{3-\delta}$ (LSCF) perovskite-type membranes: experimental study and mathematical modelling. *Ind Eng Chem Res.* 2012;51:3069–80.
31. Malavasi L, Ritter C, Chiodelli G. Correlation between thermal properties, electrical conductivity and crystal structure in the $\text{BaCe}_{0.8}\text{Y}_{0.2}\text{O}_{2.9}$ proton conductor. *Chem Mater.* 2008;20:2343–51.
32. Ding Y, Li Y, Huang W. The role of Ba concentration on the structural characteristics and electrical conductivities of $\text{Ba}_x\text{Ce}_{0.9}\text{Y}_{0.1}\text{O}_{3-x}$. *Mater Res Bull.* 2017;205:122–8.
33. Nguyen NTQ, Yoon HH. Preparation and evaluation of $\text{BaZr}_{0.1}\text{Ce}_{0.7}\text{Y}_{0.1}\text{Yb}_{0.1}\text{O}_{3-\delta}$ (BZCYYb) electrolyte and BZCYYb-based solid oxide fuel cells. *J Power Sources.* 2013;231:213–8.
34. Sun Z, Fabbri E, Bi L, Traversa E. Electrochemical properties and intermediate-temperature fuel cell performance of dense yttrium-doped barium zirconate with calcium addition. *J Am Ceram Soc.* 2012;95:627–35.
35. He B, Zhang L, Zhang Y, Ding D, Xu J, Ling Y, Zhao Y. New insight into highly active cathode of proton conducting solid oxide fuel cells by oxygen ionic conductor modification. *J Power Sources.* 2015;287:170–6.
36. Zhao L, Li G, Chen K, Ling Y, Cui Y, Gui L, He B. $\text{Sm}_{0.5}\text{Sr}_{0.5}\text{CoO}_{3-\delta}$ infiltrated $\text{Ce}_{0.9}\text{Gd}_{0.1}\text{O}_{2-\delta}$ composite cathodes for high performance protonic ceramic fuel cells. *J Power Sources.* 2016;333:24–9.